2018 IEEE International Conference on Robotics and Automation (ICRA)
May 21-25, 2018, Brisbane, Australia

Screw-Powered Propulsion in Granular Media: An Experimental and Computational Study

Andrew Thoesen[1] Sierra Ramirez[1] and Hamid Marvi[1]

***Abstract*— Screw-Propelled Vehicles (SPV's) have been widely used for terrestrial applications such as transportation over mud, snow, and amphibious environments. Similar vehicles have also been applied to industrial processes such as dewatering. Typical designs rely on a large pontoon shaft and relatively small blades to prevent unwanted sinkage or blade damage. These types of vehicles were considered during the design of the first lunar rover, given their success in aqueous and arctic media and simplicity compared to tracked vehicles. Studies have looked at the mobility of SPV's on the surface of granular media but there are not any computational and experimental studies on propulsive buried screws. Understanding the role of screw design and its angular velocity on thrust force is key to the advancement and control of SPV's. This study presents experimental and computational results of a submerged, double-helix Archimedes screw generating propulsive force against a bed of soda-lime glass beads. Thus, this research forms the basis for design of a future miniaturized exploration vehicle for space applications. In our study, we used two different screw designs (5 cm radius, 10 cm length, 63 and 44 degrees helix angle corresponding to 4 cm and 8 cm pitch, respectively) submerged in 2mm glass beads (90% roundness with sizes 1.8 mm to 2.2 mm). For both screws, a similar trend is observed between rotational speed and thrust force. We used EDEM, a Discrete Element Modeling (DEM) software for computational studies of the screw interactions with granular media. There is 5-20% discrepancy between our computational and experimental results. We will discuss possible sources of error and the potential for using DEM as a design tool for SPV's.**

I. INTRODUCTION

As early as the 1960's, screw-propelled vehicles were being investigated for use on Earth in unstable or uncertain environments [1]. Advancements have been made in land, water, and air mobility but granular or colloidal terrain is an area which has eluded us. One early example for SPV's was the Marsh Screw Amphibian. This craft propelled itself through water and then quickly transitioned to a solid, muddy environment. Another vehicle is the Amphirol. This vehicle is capable of navigating through sticky wet clays, a nearly impossible task for other forms of transportation. These extreme and unique environments require similar design considerations to the unpredictable surfaces of moons and asteroids. Many small bodies in the solar system are covered with a loose granular media called regolith. This regolith is hard to characterize from a distance but many studies estimate small grain sizes of no larger than a few millimeters [41]. The terramechanic solution of how to navigate such a material is a challenge.

*This work was supported by funding provided by Arizona State University.

[1] School for Engineering of Matter, Transport, and Energy, Arizona State University, Tempe, AZ 85287, USA hmarvi@asu.edu

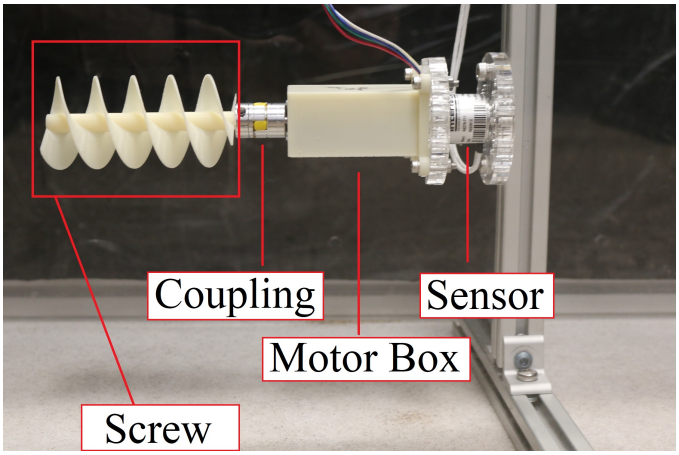

Fig. 1. Experimental setup

The most popular development of asteroid mobility has been in the form of hoppers [13]. One famous example is the MINERVA attachment to the Hayabusa mission [6] or the new generation HEDGEHOG or HOPTER [12], [15]. These approaches necessarily favor a lack of reliance on gravity from a mobility perspective. They are often found to be simple and energy efficient forms of transportation due to the low gravity of the body. The drawback is that they are less controllable and cannot perform navigation in the true sense that a ground craft would be able to.

Other approaches focus on peristaltic or waveform motion in granular media as found in snakes and worms [10], [11], [16], [17], [18], [19]. These may be energy intensive forms of motion and ineffective at moving desired distances. Recent developments have also focused on gripping and limbed control on possible asteroid surfaces. Microspine grippers [7] have been shown to be able to hang from rocky surfaces [8] and even obtain core samples without gravity assistance [9]. Unfortunately, these techniques are inapplicable to the granular media shown to cover many small body surfaces. Development in asteroid anchoring technology such as ATHLETE [14], [20] may allow examination of one spot or possibly several tangential spots but this still only allows a fraction of the terrain available for a mobile craft. Miniatured flagella-driven robots have been developed for viscous environments [34], [35], [36], a somewhat similar setting, but it is unclear how both flagella propulsion and control schemes would translate to a vacuum, granular environment. Single shaftless helix robots [37] have showed some promise in this area, as have clam-inspired agitation techniques in burrowing robots [38]. Screw-propelled vehicles have also

been explored with space context in mind [39] but without development of simulation such as DEM to explore designs in reduced gravity.

It is essential to evaluate the differences between DEM software and experimental results specifically with regards to screw propulsion in granular media. First, we must evaluate performance of the propelling screws in a well characterized environment. For this experiment, we've chosen Earth gravity and spherical glass beads of uniform size to minimize additional variables. In doing so we can begin to build a framework for more extensive design evaluation of screw propelled vehicles in simulant materials and under different gravities.

II. Experiments

Experiments were conducted in a bed of glass beads as seen in Fig. 1. To begin, two 3D printed Acrylonitrile Butadiene Styrene (ABS) screws with dimensions of 10 cm axial length by 5 cm diameter were created as seen in Fig. 2.

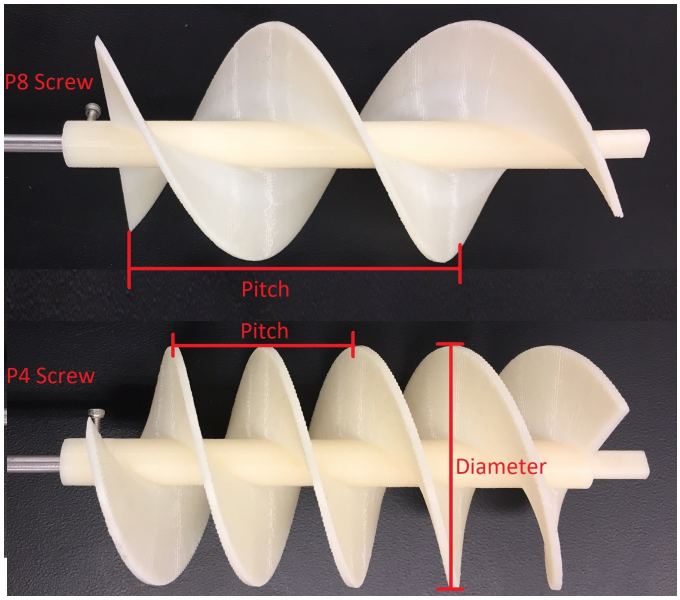

Fig. 2. 3D printed screws used for the experiments

Pitches of 4 cm and 8 cm were used. These screws will be referred to as P4 and P8 respectively henceforth. The ABS plastic screw was driven by a 12 V Pololu motor housed inside a motor casing. A shaft collar was used to connect the motor and screw. The back cover of the motor casing was then attached to a 6 DOF load cell. The motor control and RPM data collection was driven by an Arduino Uno. The experimental area of beads was 20 cm wide, 100 cm in length, and 20 cm deep.

2 mm glass beads were added to a depth up to the edge of the horizontal screw. The surface level of beads were smoothed for each trial. Each trial ran for approximately 15-20 seconds to ensure steady state values. Both P4 and P8 screws were used in all trials. Six speeds were used: 30, 45, 60, 75, 90, and 105 RPM. Ten trials were run for each speed resulting in 60 data points for each experiment.

III. Simulations

In contrast to continuum mechanics and resistive force theory, in DEM each individual particle is modeled as to affect the other particles [3], [4]. In this study, a DEM software, EDEM was employed to evaluate how well it could match experimental results and provide design insight. Within the EDEM software are different physics models which can be selected based on need. Hertz-Mindlin model is a model built on Hertzian contact theory with modifications to allow for tangential forces, damping, and friction forces (Eqs. 1-3).

$$F_n = \frac{3}{4} E^* \sqrt{R^*} \delta_n^{\frac{3}{2}} \tag{1}$$

$$\frac{1}{R^*} = \frac{1}{R_i} + \frac{1}{R_j} \tag{2}$$

$$\frac{1}{E^*} = \frac{1 - v_i^2}{E_i} + \frac{1 - v_j^2}{E_j} \tag{3}$$

In this model, the normal contact forces, F_n are functions of the specific Young's modulus, E^*, the radii of particles contacting, R^*, and the overlap, δ_n. The specific Young's modulus is derived from the particle Young's moduli, E_i and Poisson's ratios, ν_i. When two particles collide, the software allows a small volume of overlap to substitute for elastic deformation. The higher the Young's modulus, the smaller the allowable deformation. Because of this, the DEM time step is a function of particle stiffness. To use the real modulus values would make DEM simulations computationally prohibitive at particles of this size. A common technique in DEM simulations is to reduce the Young's Modulus by several orders of magnitude. A reduction of magnitude by 100 results in 10 times faster simulation times in this case [29]. Currently, our hardware produces one simulation-second per three hours with the reduced Young's modulus; one simulation-second every 30 hours would be prohibitive.

It is noted that static bulk behavior such as angle of repose for glass particles does not change significantly until Young's Modulus is in the 1E6 range [5]. However, there is a possibility of change in particles flow behavior with such a modification. During our tests of glass particles, it took significantly less energy to penetrate simulated beads of glass during calibration tests than real world counterparts. To compensate for less stiff particles, it is common practice with DEM simulation-experiment comparisons to raise one of the friction values, particularly, the particle-particle coefficient of static friction or the particle-wall coefficient of static friction [25], [30], [31], [32], [33]. There are six mechanical properties which influence the simulated flow patterns. Three properties are inherent to the material regardless of interactions: the density, Young's Modulus, and Poisson's Ratio. These parameters are well-established for soda-lime glass [27]. Although the manufacturing method of ABS affects the mechanical properties of the plastic, recent tests have established baselines for 3D-printed ABS parts [28].

The three remaining properties are interaction-dependent. They are coefficient of restitution, static friction, and rolling

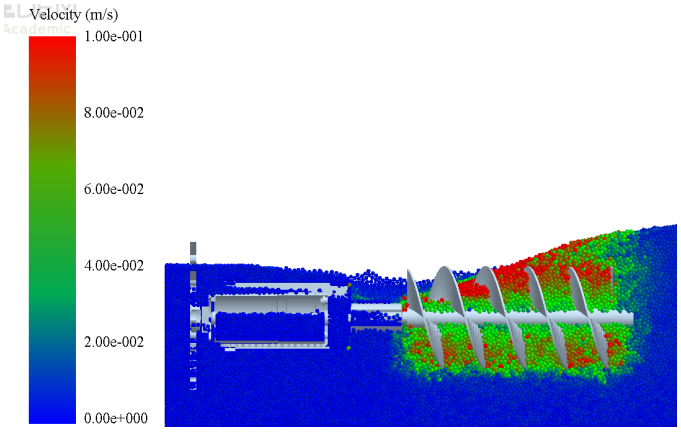

Fig. 3. A 3D model of the setup including the screw, load cell, and the frame submerged in glass beads. Particle velocities are color coded in this figure according to legend.

friction. Several experimental studies have looked at glass-glass interactions with beads of comparable size to ours (3 mm diameter) [23], [24], [25]. One experiment specifically examined coefficient of restitution with isolated bead collisions taken from high-speed camera tests, estimating the value at 0.97 [23], [24] for collision speeds under 1 m/s. This paper also gives the dynamic coefficient of friction as 0.092 and static as somewhere between 0.16-0.29. We performed our own measurement of glass-glass static friction and found values similar to the lower end at 0.16. The rolling friction coefficient of glass beads against each other has also been found to be 2.5E-5 [25].

Glass-ABS interaction properties are not reported in the literature. However, the coefficient of restitution of several different 3D-printed materials has been tested at various speeds between plastic plates and an aluminum rod [21]. The impact speeds are comparably low (below 0.5 m/s) and impactor action similar, hence the value of 0.7 was selected. Both the coefficient of static friction and the coefficient of rolling friction for glass-ABS interactions required additional experimentation. For static friction, a simple tilt test with electronic angle measurement was utilized. Static friction was estimated at 0.16, similar to the glass-glass interaction. For the coefficient of rolling friction or rolling resistance, a standardized ASTM rolling friction test was adapted [26]. Glass beads were allowed to roll from a height approximately 13 mm high. This resulted in a rolling friction of 0.173.

All of these values were input into the EDEM simulation. The simulation was set up with the real geometry of the experimental apparatus imported into EDEM as seen in Fig. 3. The same Solidworks files used to print the screws and motor box were used for the simulation. These geometries were then placed inside a cylindrical simulation bed. The simulated environment was then filled with 2 mm spherical particles. These particles were polydispersed in a normal distribution with standard deviation of 0.1 mm per the manufacturer's specifications and communication. They were also given a 1.1 aspect ratio to eliminate perfect sphericity to correlate with the 90% roundness. The degree of eccentricity has minor influence, but change from perfect spheres to 1.1 aspect ratio has been shown [40] to have a significant effect on flow patterns and force resistance. The particles were allowed to settle until movement was no longer observed. The screw was then engaged at each rotational velocity instantaneously. It was run until steady state was observed, a time of 7.5 seconds for all samples.

IV. Results

The results for axial force as a function of RPM are shown in Fig. 4 and Fig. 5. Note that the standard error of the data has been included but is too small to be seen on the graph for most data points.

It can be seen that the experimental data show a similar relationship between force and rotational velocity when compared to simulation counterparts for both the P4 and P8 screws. The simulation results are with a 3400 times reduced Young's modulus (20 MPa) while the experiment results are the mean of the ten trials for each speed.

The average thrust force error between experiment and simulation was 16% for P4 and 10.6% for P8. The absolute difference between maximum and minimum force for P4 was 0.62 N for simulation and 0.42 N for experiment. The absolute difference between maximum and minimum force for P8 was 0.49 N and 0.36 N for simulation and experiment, respectively.

While there is some variation, it seems that within the operating band of 30-105 RPMs, static craft thrust force generation could be reliably predicted in this media using DEM even with decreased Young's Modulus in the simulation.

V. Discussion

Both screws appear to have a linear trend of similar slope at lower RPM's. Indeed, the difference between 30 and 60 RPM on P4 is 0.37 N while the P8 difference is 0.33 N. This begins to taper off at higher speeds and plateau. This is likely explained by the mass flow rate balance. The cylindrical control volume of the screws can be divided into a series of "chambers" based on one full revolution around the screw. We can then examine the mass flow rate of this control volume at steady state force:

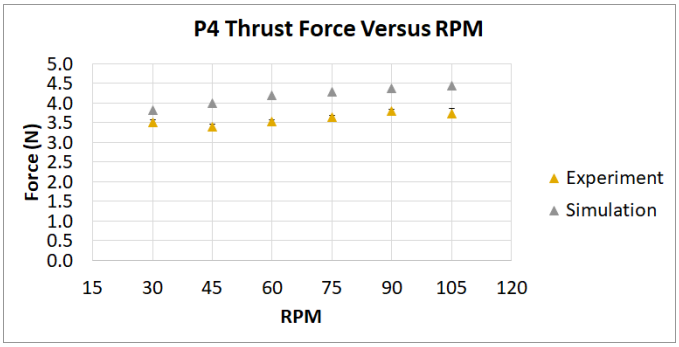

Fig. 4. Experimental and computational results for thrust force versus screw rotational velocity of P4 screw

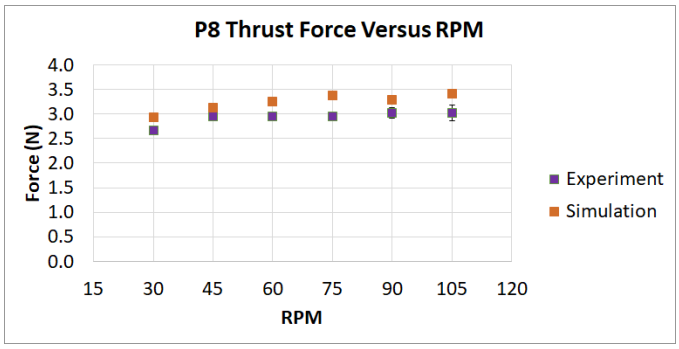

Fig. 5. Experimental and computational results for thrust force versus screw rotational velocity of P8 screw

$$\dot{m}_{in} - \dot{m}_{out} = 0 \tag{4}$$

$$\dot{m}(\phi) - \dot{m}(RPM) = 0 \tag{5}$$

$\dot{m}(\phi)$ is the mass flow rate of beads falling in to the screw control volume due to exceeding angle of repose; it is a function of material properties. $\dot{m}(RPM)$ is the mass flow rate out of the screw control volume as a function of rotational speed; it is the beads being pushed out. At any speed, the steady state force in the control volume of a screw is subject to these two mass flow rates as seen in Eqs. 4 and 5.

According to Eq. 5, the mass flow rate out of the volume is the action of the screw converting radial movement to axial and pushing particles out. For this discussion, two properties are the key factors. A faster RPM will typically discharge more particles. A larger pitch will generate more movement vertically rather than horizontally. However, the axial velocity compared to radial velocity will be larger and thus discharges more particles. This discussion assumes a screw submerged with the blades tangential to surface level. As a screw removes particles, it creates a void. With a sufficiently large volume of particles and slopes steeper than the angle of repose, new particles will move to fill this void. This refill rate is a function of gravity and the angle of repose.

The control volume will eventually reach a steady state at any RPM where the refill rate is balanced with the rate of particles being pushed out of the control volume. This produces the steady state, RPM-dependent force for a particular design. As previously stated, the mass flow out rate for a constant screw design is RPM dependent. The maximum mass flow in rate into the volume is bounded by granular material properties; if the gravity is too low or the angle of repose too steep, particles will not move quickly enough to fill in voids. Since the control volume must be balanced at steady state then this implies the maximum mass flow out rate is bounded as well and there is a maximum force for each screw design and set of material properties. As a particular screw approaches the maximum limit RPM in a particular material, potential force gains from increased speed are negated by decreased mass within each chamber, since the material will not fill the control volume quickly enough. This explains the behavior of the later RPMs in both simulation and experimentation. Both screws eventually reach a maximum force threshold. If the screws were moving in a homogeneous environment, it would undoubtedly introduce more material for the screw to push against since the control volume would consistently move. The screws would then increase velocity until the propulsive force was equal to the drag force. The screw shape is such that it can move through a fluidic environment with little resistance, so its linear velocity would be estimated by the pitch and rotational velocity. That is if our P4 screw were rotating at one revolution/second, it would move linearly at a rate of approximately 4 cm/s. The bigger limiting factor would likely be the drag coefficient of whatever craft it was attached to. This idea is explored in the future works section.

We can also compare the simulation and experimental results to similar situations in the literature [22]. As previously mentioned, when Young's Modulus reduction was suggested [5] it was cautioned about the possibilities of geometry forces being reduced. Many of the comparative papers look at the flow and collapse patterns of tumbling drums or piling features. In such a setup, while particles are piled they are not as forced or pressed against each other by geometries; the deformation is not as crucial of a feature. This, along with experimental error, is likely the source of difference between simulation and experiment. The takeaway is that Young's modulus reduction is acceptable for simulations where particle compression against screw geometries is a feature of the flow. We can examine a simulation closer to the real value, compare to forces generated by a low value one, and use that difference in force as an estimated adjustment for simulation predictions.

VI. Future Work

We would like to use the experimental and computational techniques discussed in this study for designing asteroid mobility systems. While we find general conformity with the results, we plan to explore further screw design parameters such as length and pitch to determine propulsion characteristics. We also plan to explore craft designs with both subsurface and surface characteristics. It is possible to vary length, number of screws, placement, and many other design factors. We also would like to move onto more realistic materials and different gravities. Glass beads were chosen for reliability of properties and common literature usage.

Moreover, we have performed preliminary simulations (Fig. 7) which show that a subsurface craft is able to maintain steady state velocity at particle density and gravity found on a small body such as Phobos. Fig. 6 shows the velocity for a 1 kg craft body at various rotational velocities of its two driving screws. The maximum velocity is 4mm/s, which is not trivial for a craft of 10 cm length. It was simulated using a coupling of MSC Adams, a multi body dynamics (MBD) package, and EDEM. By refining our approach, we can utilize MBD-DEM modeling to assess the design of such a craft. We have recently obtained BP-1 lunar simulant from NASA and are exploring the possibility of similar tests in it.

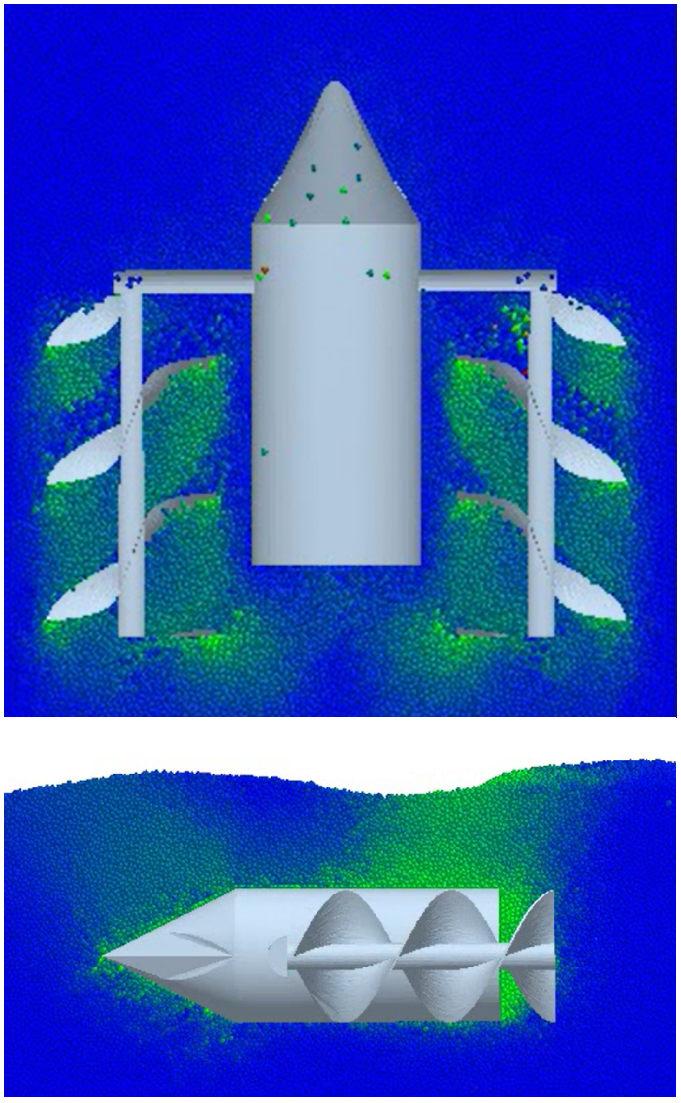

Fig. 6. Simulation of screw-powered craft in Phobos gravity. Color warmth scale is identical to Fig. 3

If we can achieve accuracy in modeling this material, it will open up new simulation options for exploratory vehicles.

VII. Conclusion

In this study, we evaluated two screw designs at six speeds with ten trials for each speed experimentally. We evaluated those same screw designs with EDEM software with adjustments to the Young's Modulus and static friction as suggested by the available literature. We found good agreement between simulation and experimental results (5-20% error). We hypothesize the reduced Young's modulus of glass beads used in the simulations and experimental measurement error contribute to this discrepancy. We also discovered the lack of sufficient particle flow in rate limits the increase in thrust force with increasing screw rotational velocity. We would like to use our experimentally verified DEM simulations to study asteroid mobility and presented some preliminary results on SPVs locomotion at micro gravity.

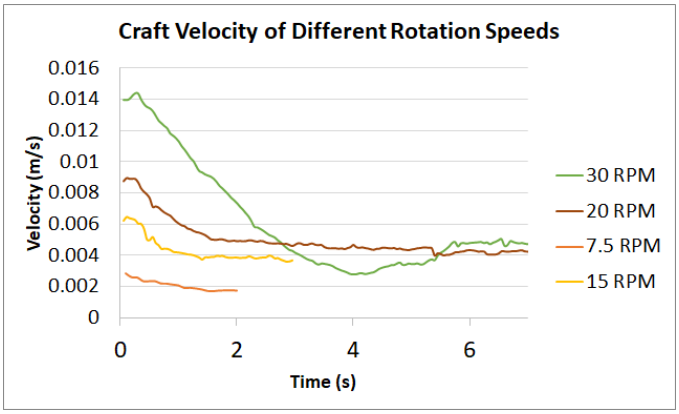

Fig. 7. Steady state velocities achieved by submerged craft

ACKNOWLEDGMENT

The authors would like to thank Professor Heather Emady and Spandana Vajrala for fruitful discussions on DEM simulations of granular media and Arizona State University for funding.

References

[1] M. J. Neumeyer, and B. D. Jones. "The marsh screw amphibian." Journal of Terramechanics 2, no. 4 (1965): 83-88.

[2] M. Ucgul, J. M. Fielke, and C. Saunders, Defining the effect of sweep tillage tool cutting edge geometry on tillage forces using 3D discrete element modelling, Information Processing in Agriculture, vol. 2, no. 2, pp. 130141, 2015

[3] H. Askari and K. Kamrin, Intrusion rheology in grains and other flowable materials, Nature Materials, vol. 15, no. 12, pp. 12741279, 2016.

[4] D. C. Motley, Physical experimentation and actuated wheel design for granular locomotion using Resistive Force Theory, Ph.D. dissertation, Massachusetts Institute of Technology, 2016

[5] S. Lommen, D. Schott, and G. Lodewijks, DEM speedup: Stiffness effects on behavior of bulk material, Particuology, vol. 12, pp. 107112, 2014

[6] A. Fujiwara, et al. "The rubble-pile asteroid Itokawa as observed by Hayabusa." Science 312.5778 (2006): 1330-1334.

[7] A. Parness, Anchoring foot mechanisms for sampling and mobility in microgravity, 2011 IEEE International Conference on Robotics and Automation, 2011

[8] A. Parness, M. Frost, N. Thatte, and J. P. King, Gravity-independent mobility and drilling on natural rock using microspines, 2012 IEEE International Conference on Robotics and Automation, 2012.

[9] A. Parness and M. Frost, Microgravity coring: A self-contained anchor and drill for consolidated rock, 2012 IEEE Aerospace Conference, 2012.

[10] H. Omori, T. Murakami, H. Nagai, T. Nakamura, and T. Kubota, Development of a Novel Bio-Inspired Planetary Subsurface Explorer: Initial Experimental Study by Prototype Excavator With Propulsion and Excavation Units, IEEE/ASME Transactions on Mechatronics, vol. 18, no. 2, pp. 459470, 2013.

[11] H. Omori, T. Murakami, H. Nagai, T. Nakamura, and T. Kubota, Validation of the measuring condition for a planetary subsurface explorer robot that uses peristaltic crawling, 2013 IEEE Aerospace Conference, 2013

[12] D. Mge, J. Gurgurewicz, J. Grygorczuk, . Winiewski, and G. Thornell, The Highland Terrain Hopper (HOPTER): Concept and use cases of a new locomotion system for the exploration of low gravity Solar System bodies, Acta Astronautica, vol. 121, pp. 200220, 2016.

[13] Reid, Robert G., et al. "Contact dynamics of internally-actuated platforms for the exploration of small solar system bodies." Proceedings of the 12th International Symposium on Artificial Intelligence, Robotics and Automation in Space (i-SAIRAS2014), Saint-Hubert, Canada. 2014.

[14] B. H. Wilcox, ATHLETE: A limbed vehicle for solar system exploration, 2012 IEEE Aerospace Conference, 2012.
[15] M. Pavone, J. C. Castillo-Rogez, I. A. D. Nesnas, J. A. Hoffman, and N. J. Strange, Spacecraft/rover hybrids for the exploration of small Solar System bodies, 2013 IEEE Aerospace Conference, 2013
[16] C. Wright, A. Buchan, B. Brown, J. Geist, M. Schwerin, D. Rollinson, M. Tesch, and H. Choset, Design and architecture of the unified modular snake robot, 2012 IEEE International Conference on Robotics and Automation, 2012.
[17] W. Zhen, C. Gong, and H. Choset, Modeling rolling gaits of a snake robot, 2015 IEEE International Conference on Robotics and Automation (ICRA), 2015
[18] H. Marvi, C. Gong, N. Gravish, H. Astley, M. Travers, R. L. Hatton, J. R. Mendelson, H. Choset, D. L. Hu, and D. I. Goldman, Sidewinding with minimal slip: Snake and robot ascent of sandy slopes, Science, vol. 346, no. 6206, pp. 224229, Sep. 2014
[19] H. Marvi, J. Bridges, and D. L. Hu, Snakes mimic earthworms: propulsion using rectilinear travelling waves, Journal of The Royal Society Interface, vol. 10, no. 84, pp. 2013018820130188, Jan. 2013
[20] A. S. Howe and B. Wilcox, Outpost assembly using the ATHLETE mobility system, 2016 IEEE Aerospace Conference, 2016.
[21] K. Kardel, H. Ghaednia, A. L. Carrano, and D. B. Marghitu, Experimental and theoretical modeling of behavior of 3D-printed polymers under collision with a rigid rod, Additive Manufacturing, vol. 14, pp. 8794, 2017.
[22] E. Alizadeh, F. Bertrand, and J. Chaouki, Comparison of DEM results and Lagrangian experimental data for the flow and mixing of granules in a rotating drum, AIChE Journal, vol. 60, no. 1, pp. 6075, 2013.
[23] Normal Collisions of Spheres: A Literature Survey on Available Experiments
[24] S. F. Foerster, M. Y. Louge, H. Chang, and K. Allia, Measurements of the collision properties of small spheres, Physics of Fluids, vol. 6, no. 3, pp. 11081115, 1994.
[25] K. Khan and G. Bushell, Comment on Rolling friction in the dynamic simulation of sandpile formation, Physica A: Statistical Mechanics and its Applications, vol. 352, no. 2-4, pp. 522524, 2005.
[26] "Standard Test Method for Measuring Rolling Friction Characteristics of a Spherical Shape on a Flat Horizontal Plane", ASTM G19408, 2013
[27] R. E. Bolz and G. L. Tuve, Handbook of tables for applied engineering science: CRC handbook of tables for applied engineering science. Cleveland,OH: Chemical rubber company, 1970
[28] B. Tymrak, M. Kreiger, and J. Pearce, Mechanical properties of components fabricated with open-source 3-D printers under realistic environmental conditions, Materials and Design, vol. 58, pp. 242246, 2014.
[29] S. Lommen, D. Schott, and G. Lodewijks, DEM speedup: Stiffness effects on behavior of bulk material, Particuology, vol. 12, pp. 107112, 2014.
[30] R. Yang, C. Jayasundara, A. Yu, and D. Curry, DEM simulation of the flow of grinding media in IsaMill, Minerals Engineering, vol. 19, no. 10, pp. 984994, 2006.
[31] N. Taberlet, M. Newey, P. Richard, and W. Losert, On axial segregation in a tumbler: an experimental and numerical study, Journal of Statistical Mechanics: Theory and Experiment, vol. 2006, no. 07, 2006.
[32] R. Stewart, J. Bridgwater, Y. Zhou, and A. Yu, Simulated and measured flow of granules in a bladed mixera detailed comparison, Chemical Engineering Science, vol. 56, no. 19, pp. 54575471, 2001.
[33] E. Alizadeh, F. Bertrand, and J. Chaouki, Comparison of DEM results and Lagrangian experimental data for the flow and mixing of granules in a rotating drum, AIChE Journal, vol. 60, no. 1, pp. 6075, 2013.
[34] I. S. M. Khalil, A. F. Tabak, Y. Hamed, M. E. Mitwally, M. Tawakol, A. Klingner, and M. Sitti, Swimming Back and Forth Using Planar Flagellar Propulsion at Low Reynolds Numbers, Advanced Science, p. 1700461, Jan. 2017.
[35] I. S. M. Khalil, A. F. Tabak, A. Klingner, and M. Sitti, Magnetic propulsion of robotic sperms at low-Reynolds number, Applied Physics Letters, vol. 109, no. 3, p. 033701, 2016.
[36] Z. Ye, S. Regnier, and M. Sitti, Rotating Magnetic Miniature Swimming Robots With Multiple Flexible Flagella, IEEE Transactions on Robotics, vol. 30, no. 1, pp. 313, 2014.
[37] B. D. Texier, A. Ibarra, and F. Melo, Helical Locomotion in a Granular Medium, Physical Review Letters, vol. 119, no. 6, Oct. 2017.
[38] K. N. Nordstrom, D. S. Dorsch, W. Losert, and A. G. Winter, Microstructural view of burrowing with a bioinspired digging robot, Physical Review E, vol. 92, no. 4, 2015.
[39] K. Nagaoka, M. Otsuki, T. Kubota, and S. Tanaka, Terramechanics-based propulsive characteristics of mobile robot driven by Archimedean screw mechanism on soft soil, 2010 IEEE/RSJ International Conference on Intelligent Robots and Systems, 2010.
[40] R. Bharadwaj, W. R. Ketterhagen, and B. C. Hancock, Discrete element simulation study of a Freeman powder rheometer, Chemical Engineering Science, vol. 65, no. 21, pp. 57475756, 2010.
[41] B. Gundlach and J. Blum, A new method to determine the grain size of planetary regolith, Icarus, vol. 223, no. 1, pp. 479492, 2013.